processes

MDPI

Article

Investigation on Safety Dynamic Evolution Mechanism of a Distributed Low Carbon Manufacturing System with Large Time Delay

Bo Liu [1], Yudie Chen [2], Hongyan Zuo [2,*], Guohai Jia [2] and Dingqing Zhong [2]

[1] School of Electrical and Information Engineering, Hunan Institute of Engineering, Xiangtan 411104, China
[2] School of Mechanical Engineering, Hunan Institute of Engineering, Xiangtan 411104, China
* Correspondence: zuohongyan@hnie.edu.cn

Abstract: In order to reveal the inducing factors and safety dynamic evolution mechanism of frequent personal injury accidents under a low carbon manufacturing process, a nonlinear safety dynamic evolution model of a distributed low carbon manufacturing system with large time delay is established. The established model is then verified by simulation results from mathematical analysis and dynamic evolution. Moreover, qualitative analysis on nonlinear safety dynamic evolution and the trend of human–machine safety under a low carbon manufacturing process is investigated. Finally, an application case of the established model is studied. The key results are as follows: (1) There are four dynamic regions, namely the safety area I, the deterioration area II, the asymptotically stable safety area III, and the enhancement area IV of the safety ability in the interaction evolution model of carelessness and safety levels; (2) There are two singularities in the dynamic evolution model of the man–machine safety system with large time delay under a low carbon manufacturing process; (3) The equilibrium points of the human–machine safety system are $E_1 = (0, 0)$ and $E_2 = (0.5333, 0.2489)$, while changes in the carelessness level have a serious block effect on safety development with time; (4) For the radial tire casing process, the low carbon development trend of the technological process of radial tire casing is good, but low carbon structure and management have slightly lower low carbon levels. This work provides a theoretical basis for the safety evaluation and control of the distributed low carbon manufacturing human–machine safety system with large time delay.

Keywords: distributed low carbon manufacturing system; low carbon manufacturing process; safety; dynamic evolution mechanism

Citation: Liu, B.; Chen, Y.; Zuo, H.; Jia, G.; Zhong, D. Investigation on Safety Dynamic Evolution Mechanism of a Distributed Low Carbon Manufacturing System with Large Time Delay. *Processes* **2022**, *10*, 1707. https://doi.org/10.3390/pr10091707

Academic Editor: Anna Trubetskaya

Received: 27 July 2022
Accepted: 24 August 2022
Published: 27 August 2022

1. Introduction

In recent years, green low carbon intelligent manufacturing has become the core technology to enhance the overall competitiveness of the global manufacturing industry [1]. Fundamentally, green and low carbon intelligent manufacturing aims to change each process of traditional manufacturing with the help of constantly developing modern advanced technology as well as create a new manufacturing form and mode. From the operating level, a synergy of mechanical properties between humans and machines in the traditional manufacturing process is developed toward a higher level of synergy of intelligence between human and machine intelligence, reducing the influence of human intelligence defects on manufacturing, and taking full advantage of machine intelligence to compensate for the lack of human intelligence. With the application of information technology and intelligent technology, the traditional operation interface and its management mode are changed, which will greatly increase the security risk of the future human–machine manufacturing system, and even contain new possible social risks. In such low carbon intelligent manufacturing systems, future security risks mainly exist at the human–machine interface level. The disconnection or careless connection between human intelligence and machine intelligence in any link may lead to the generation and spread of risks in the

entire manufacturing system, leading to the collapse of the system. Therefore, a low carbon intelligent manufacturing system is a highly complex human–machine cooperation system. Cooperation and safety problems are the main problems faced by the system, with effective human–machine cooperation an important guarantee to ensure the safety and efficiency of the system [2]. It is necessary to investigate the human–machine safety system under a low carbon manufacturing process.

Safety is regarded as a major obstacle for introducing human–robot collaboration in industrial production. There are some studies that have contributed to human–machine safety. For example, on the basis of Human Cyber Physical fusion intelligence, Liu et al. [3] discussed the mechanism of an intelligent manufacturing system with HCP fusion and collaboration, and explored the HCP data fusion mechanism, collaboration mechanism, and interaction mechanism. For concurrent simultaneous consideration of the reliability and safety of manufacturing systems, as well as flexibility and performance, a specialized control architecture was proposed by Ding et al. [4]; they extended the architecture by a specific technique for the strategic controller. For the case of an intelligent manufacturing system which reacts adaptively to a human operator, control trajectories for a robot arm are computed online such that collision with the operator is excluded. The computation is based on solving a mixed-integer programming problem that takes a dynamic safety area around the operator into account as a constraint. Human–machine interaction (HMI) safety for cyber–physical systems is critical and its analysis is mandatory in many domains such as SCADA, autonomous cars, and medical devices. The generation of dynamic accident scenarios is the cornerstone of safety analysis. Fan et al. [5] presented a platform and associated methodology to effectively generate accident scenarios by modeling HMI errors using model-level fault injection, followed by simulation to produce dynamic evolutions of accident scenarios. Results showed that human mode confusion triggered by false displays may lead to severe accidents. In the study by Hanna et al. [6], the difference between traditional collaborative robots and intelligent human–robot collaboration was analyzed and a new safety approach, named Deliberative Safety, was suggested, allowing humans and robots to switch between different safety measures based on the need for flexibility or efficiency to reach production goals. While considering system performance, a taxonomy was proposed to better support the design of deliberative safety. Five safety measures were used in a deliberative safety approach, including perimeter safety, zone safety, reactive safety, planned safety, and active safety, and when used together, they can enable intelligent human–robot collaboration.

For safety studies under a low carbon manufacturing process from previous works, the static safety evaluation method [7] was used to show that the safety index is in a certain range, but it cannot be used to reveal the real dynamic evolution rule of safety under low carbon manufacturing process. Obviously, the static safety evaluation method can easily cause the inconsistent phenomena where static safety evaluation and safety trend do not coincide with accident rate in the practical process. The dynamic evolution theory [8–10] is a nonlinear, dynamic, and unbalanced evolution process theory [11] which is based on the nonconstructive, nonhuman design principles of rational evolution [12,13] and applied in vehicle road safety [14], reactor safety [15], lithium-ion pouch cells safety [16], automated terminals safety [17], etc., but this theory has not been employed in safety evaluation of the low carbon manufacturing system. In a low carbon intelligent manufacturing system, there is a highly complex and dynamic human–machine cooperation in the human–machine interface, though safety dynamic evolution of the inducing factors from human and equipment can lead to the generation and spread of risks in the system. Therefore, it is critical to effectively reveal the inducing factors of frequent personal injury accidents resulting from mechanical equipment problems or human problems under a low carbon manufacturing process. The human–machine safety engineering principle provides a very good idea about knowing the frequent personal injury phenomenon from the viewpoint of a system [18,19], effectively overcoming one-sidedness shortcomings [20,21] and putting forward feasible safety countermeasures. In addition, human carelessness with time delays

will have an effect on safety in the low carbon manufacturing process; namely the effects on safety caused by human carelessness will be shown after a certain period of time.

Therefore, the large time delay must be considered when a dynamic evolution model of human–machine safety is established by taking advantage of time delay differential formula theory [22–25]. In this paper, human factors for safety accidents under the distributed low carbon manufacturing process are firstly analyzed. A safety–careless dynamic evolution model of a distributed low carbon manufacturing system with large time delay is then established. Finally, low carbon level evaluation of a human–machine safety system under a low carbon manufacturing process and an application case of this dynamic evolution model are investigated. This work will provide a theoretical basis for the safety evaluation and control of the human–machine safety system under a low carbon manufacturing process.

2. Theoretical Framework

2.1. Human Misjudgments Caused by Unidirectional Transmission of Information Channel

The information transmission of the man–machine safety system under a low carbon manufacturing process is unidirectional so that there is no information feedback from machine subsystem to human subsystem when the orders are issued from human subsystem to machine subsystem [26].

When a machine subsystem is used in case of failure, the single loop network structure of the man–machine system will cause a human subsystem under low carbon manufacturing process to experience adverse conditions:

(a) The speed of information processing will be greatly reduced; (b) There will be a loss of ability to judge and process more than two malfunctions' information simultaneously; (c) Human subsystems will be so confused that the varieties of judgment in emergencies cannot be handled; (d) The "software" of the human brain system in the human subsystem under a low carbon manufacturing process naturally falls into "moronism" states when suddenly encountering abnormal situations and danger anomalism.

Therefore, the human subsystem experiencing adverse conditions will result in serious safety accidents [27] under low carbon manufacturing process. Most of the safety accidents under low carbon manufacturing process are caused by unsafe behavior from the human subsystem.

2.2. Loss of Human Alertness in Human–Machine Safety System

Obviously, thinking, judgment, and information processing must be matched with specific human–machine safety conditions in the operation process of the human subsystem under a low carbon manufacturing process. The so-called loss of human alertness means that the specific environment of the human–machine safety system is forgotten by the human subsystem. As for the production site, with the influence of noise without governance, as well as hot and humid environment factors, operators who work 4~5 h continuously every day will inevitably experience monotony and be extremely vulnerable to psychological and physical fatigue, with some phenomena being a decreased consciousness level of the brain, lax operating attention, and frequent mis-operation.

According to an analysis of the human subsystem under a low carbon manufacturing process, the human subsystem will generate simultaneous effects psychologically and physically because of the continuous and monotonous noise, with almost the same frequency vibration behavior under a low carbon manufacturing process. Once the machine subsystem stops working, the psychology of the human subsystem will be in imbalance, resulting in a loss of alertness of the human subsystems and leading to eventual mistakes in the human subsystem.

3. Safety–Careless Dynamic Evolution Model of a Distributed Low Carbon Manufacturing System with Large Time Delay

3.1. Establishment of the Dynamic Evolution Model

When the operators of a human–machine safety system under low carbon manufacturing process feel high safety, they will tend to be relaxed and the safety of the human–machine safety system under a low carbon manufacturing process will finally decrease. On the contrary, when the operators of the man–machine system under low carbon manufacturing process feel low safety, the tight nerve will reduce the carelessness of the man–machine safety system. That is, the safety and carelessness of the human–machine safety system under a low carbon manufacturing process are two nonlinear correlated variables which are mutually affected.

In order to establish a dynamic evolution model of the human–machine safety system with large time delay under a low carbon manufacturing process, the following assumptions can be made.

(1) Based on the safety theory [28–30], the safety level and carelessness level of the human–machine safety system under a low carbon manufacturing process are denoted as $x(\tau)$ and $y(\tau)$, respectively, and also satisfy the following conditions:
   (a) A higher value of $x(\tau)$ shows that the safety level of the human–machine safety system under a low carbon manufacturing process is higher, while a lower $x(\tau)$ shows a lower safety level of the human–machine safety system under a low carbon manufacturing process.
   (b) The higher the $y(\tau)$ value, the lower the alertness of the human–machine safety system under a low carbon manufacturing process, resulting in higher thought slackness and a higher degree of careless behavior; on the contrary, the lower the value of $y(\tau)$, the higher the alertness of the human–machine safety system under a low carbon manufacturing process, leading to lower thought slackness and a lower degree of careless behavior.

(2) The intrinsic growth rates of the safety level and carelessness level of the human–machine safety system under a low carbon manufacturing process are denoted as a_1 ($a_1 > 0$) and b_1 ($b_1 > 0$), respectively.

(3) The threshold values of the safety level and carelessness level of the human–machine safety system under a low carbon manufacturing process are M ($M > 0$) and m ($m > 0$), respectively, with $m < M$.

Given that the influence of the carelessness level on safety level is of the time delay τ_0, the influence value of the carelessness level $y(\tau)$ on the safety level evolution speed $\mathrm{d}x(\tau)/\mathrm{d}\tau$ can be expressed as $-a_2 y(\tau - \tau_0)$ at time τ. At the same time, the safety state evolution speed $\mathrm{d}x(\tau)/\mathrm{d}\tau$ at time τ is affected by the safety level $x(\tau)$ and safety level change trend $[1 - x(\tau)/M]$; thus, the safety state evolution speed $\mathrm{d}x(\tau)/\mathrm{d}\tau$ under a low carbon manufacturing process can be expressed as:

$$\frac{\mathrm{d}x(\tau)}{\mathrm{d}\tau} = a_1 \cdot x(\tau)[1 - \frac{x(\tau)}{M}] - a_2 \cdot y(\tau - \tau_0) \quad (1)$$

where a_2 is the influence coefficient of the carelessness level on the safety level and $a_2 > 0$.

Formula (1) shows that the intrinsic growth a_1 of the safety level can effectively describe the linear relationship between growth speed of the safety level and the real-time safety level as well as the change trend of the safety level; the greater the intrinsic growth a_1 is, the greater the coupling influence of the safety level and the change trend of the safety level on the growth speed of the safety level is. Moreover, the influence coefficient a_2 of the carelessness level on the safety level can better describe the linear relationship between the growth rate of the carelessness level and the growth rate of the safety level, with the greater the influence coefficient a_2 is, the greater the influence of carelessness on safety is.

In addition, the influence of the carelessness level $y(\tau)$ on carelessness level evolution speed $\mathrm{d}y(\tau)/\mathrm{d}\tau$ at time τ can be expressed as $-b_2 y(\tau)$, while the influence of the safety level

$y(\tau)$ on evolution speed $dy(\tau)/d\tau$ of the carelessness level at time τ can also be expressed as $b_1[m - x(\tau)]x(\tau)$. Therefore, the evolution speed $dy(\tau)/d\tau$ of the careless state under a low carbon manufacturing process can be expressed as:

$$\frac{dy(\tau)}{d\tau} = b_1 \cdot x(\tau)[m - x(\tau)] - b_2 \cdot y(\tau) \quad (2)$$

where b_2 is the resistance coefficient and $b_2 > 0$.

Formula (2) show that the intrinsic growth b_1 of the carelessness level can be used to effectively describe the linear correlation between the growth speed of carelessness and other factors such as the threshold value m of the carelessness level and the difference of the safety level $x(\tau)$.

When $x(\tau)$ is less than m, the safety of the human–machine safety system under a low carbon manufacturing process is insufficient, with the carelessness level increasing with the growth of the safety level, $x(\tau)$. When $x(\tau)$ is greater than m, the safety of the human–machine safety system under a low carbon manufacturing process is fully strengthened, with the carelessness level decreasing with the growth of the safety level $x(\tau)$. In addition, the resistance coefficient b_2 can be used to effectively describe the negative linear relationship between the growth speed of the carelessness and alertness level of the personnel; namely the higher the carelessness, the slower the growth of the carelessness level.

The mathematical models shown in Formulas (1) and (2) can be used to effectively describe the dynamic evolution relationship and rule between the safety and carelessness levels under a low carbon manufacturing process.

Setting $u(\tau) = x(\tau)/M$, $v(\tau) = y(\tau)/M$, and $a_2 \cdot t = \tau$, Formulas (1) and (2) can be reformulated as:

$$\begin{cases} \frac{du(\tau)}{d\tau} = \frac{a_1}{a_2} \cdot u(\tau)[1 - u(\tau)] - v(\tau - \tau_0) \\ \frac{dv(\tau)}{d\tau} = \frac{b_1 M}{a_2} \cdot u(\tau)[\frac{m}{M} - u(\tau)] - \frac{b_2}{a_2} \cdot v(\tau) \end{cases} \quad (3)$$

Setting $a = a_1/a_2$, $b = b_2/a_2$, $c = b_1 \cdot M/a_2$, and $d = m/M$, changing τ into t, and making $u(\tau) = u(t)$ and $v(\tau) = v(t)$, then the ordinary differential Formula (3) can be reformulated as:

$$\begin{cases} \frac{du(t)}{dt} = a \cdot u(t)[1 - u(t)] - v(t - t_0) \\ \frac{dv(t)}{dt} = c \cdot u(t)[d - u(t)] - b \cdot v(t) \end{cases} \quad (4)$$

The ordinary differential formulas shown in Formula (4) are of the topology homeomorphism phase diagram with the ordinary differential Formulas (1) and (2).

3.2. Mathematical Analysis of the Dynamic Evolution Model with Large Time Delay

Assuming that $(a_1 + b_2)^2/(4a_2b_1) < m < M$ (namely $(a + b)^2/(4c) < d < 1$) is always correct, the dynamic evolution model of the human–machine safety system with large time delay under a low carbon manufacturing process can be analyzed by the mathematical method shown in Formula (4).

Lemma 1. *If there is $a \leq b$ in ordinary differential Formula (4), then there is not closed rail in ordinary differential Formula (4); that is, ordinary differential Formula (4) is not of periodic solution.*

Lemma 2. *Ordinary differential Formula (4) has two finite singular points, namely (0, 0) and (u_0, v_0) (including $u_0 = (ab - cd)/(ab - c)$ and $v_0 = cu_0(d - u_0)/b$); (u_0, v_0) belongs to the first quadrant and is a saddle point, while (0, 0) is stable course focusing ($a < b - t_0cd$).*

Based on Lemma 2, the ordinary differential formula shown in Formula (4) is of two **finite singular points**, namely $E_1 = (0, 0)$ and $E_2 = (u_0, v_0)$ (including $u_0 = [(ab - cd)/(ab - c)] > 0$

and $v_0 = [cu_0(d - u_0)/b] > 0$), so the first approximation system of the ordinary differential Formula (4) at stable points E_1 and E_2 can be expressed as follows:

$$\begin{cases} \frac{du(t)}{dt} = a \cdot u(t) - v(t - t_0) \\ \frac{dv(t)}{dt} = c \cdot d \cdot u(t) - b \cdot v(t) \end{cases} \tag{5}$$

$$\begin{cases} \frac{du(t)}{dt} = a(1 - 2u_0)u(t) - v(t - t_0) \\ \frac{dv(t)}{dt} = c(d - 2u_0)u(t) - bv(t) \end{cases} \tag{6}$$

The characteristic equations of Formulas (5) and (6) are **described by** Formulas (7) and (8), respectively.

$$\begin{vmatrix} \lambda - a & -\exp(-\lambda t_0) \\ cd & \lambda - (-b) \end{vmatrix} = 0 \tag{7}$$

$$\begin{vmatrix} \lambda - a(1 - 2u_0) & -\exp(-\lambda t_0) \\ c(d - 2u_0) & \lambda - (-b) \end{vmatrix} = 0 \tag{8}$$

The solutions of the characteristic equations shown in Formulas (7) and (8) can be expressed as follows:

$$\lambda^2 + (b - a)\lambda - ab + cd\exp(-\lambda t_0) = 0 \tag{9}$$

$$\lambda^2 + [b - a(1 - 2u_0)]\lambda - ab(1 - 2u_0) + c(d - 2u_0)\exp(-\lambda t_0) = 0 \tag{10}$$

Theorem 1.

(a) When $t_0 = t_{c1}$, characteristic Equation (9) is of two pure imaginary roots: $\pm\omega_{c1}i$, including:

$$\omega_{c1} = \sqrt{-\frac{a^2 + b^2}{2} + \frac{1}{2}\sqrt{(a^2 + b^2)^2 - 4(a^2b^2 - c^2d^2)}}$$

$$t_{c1} = \frac{1}{\omega_{c1}}\left(\arccos\frac{\omega_{c1}^2 + ab}{cd} + 2\pi j\right), \quad j = 0, 1, \ldots$$

(b) When $2cd > c + ab$ and $t_0 = t_{c2}$, characteristic Equation (10) is of two pure imaginary roots: $\pm\omega_{c2}\boldsymbol{i}$, including:

$$\omega_{c2} = \sqrt{-\frac{a^2(1 - 2u_0)^2 + b^2}{2} + \frac{1}{2}\sqrt{\left[a^2(1 - 2u_0)^2 + b^2\right]^2 - 4\left[a^2(1 - 2u_0)^2b^2 - c^2(d - 2u_0)^2\right]}}$$

$$t_{c2} = \frac{1}{\omega_{c2}}\left[\arccos\frac{\omega_{c2}^2 + a(1 - 2u_0)b}{c(d - 2u_0)} + 2\pi j\right], \quad j = 0, 1, \ldots$$

Proof.

(a) Assume that ωi (including $\omega > 0$) is a root of characteristic Equation (9), then,

$$-\omega^2 + (b - a)\omega\boldsymbol{i} - ab + cd(\cos\omega t_0 - \boldsymbol{i}\sin\omega t_0) = 0 \tag{11}$$

The real part and imaginary part of Formula (11) can be separated as Formulas (12) and (13).

$$-\omega^2 - ab + cd\cos\omega t_0 = 0 \tag{12}$$

$$(b - a)\omega - cd\sin\omega t_0 = 0 \tag{13}$$

Because $\cos^2\omega t_0 + \sin^2\omega t_0 = 1$, Formulas (12) and (13) can then be reformulated as Formula (14).

$$\omega^4 + (a^2 + b^2)\omega^2 + a^2b^2 - c^2d^2 \tag{14}$$

The root $\omega^2 < 0$ for Formula (14) should be rejected according to the practical meaning, then:

$$\omega^2 = -\frac{a^2+b^2}{2} + \frac{1}{2}\sqrt{(a^2+b^2)^2 - 4(a^2b^2 - c^2d^2)} \tag{15}$$

Obviously, if Formula (15) is correct, then an inequality such as $\frac{1}{2}\sqrt{(a^2+b^2)^2 - 4(a^2b^2 - c^2d^2)} - \frac{a^2+b^2}{2} > 0$ is also correct. Therefore, the proof problem of Formula (15) can be transformed as the proof problem of Formula (16).

$$\sqrt{(a^2+b^2)^2 - 4(a^2b^2 - c^2d^2)} > a^2 + b^2 \tag{16}$$

Formula (16) can be reformulated as follows:

$$(a^2+b^2)^2 - 4(a^2b^2 - c^2d^2) > (a^2+b^2)^2 \Leftrightarrow 4(c^2d^2 - a^2b^2) > 0 \Leftrightarrow cd > ab$$

Based on known condition that $u_0 = [(ab - cd)/(ab - c)]$ is greater than 0, then **an** inequality such as $cd > ab$ is concluded, so an inequality such as $\frac{1}{2}\sqrt{(a^2+b^2)^2 - 4(a^2b^2 - c^2d^2)} - \frac{a^2+b^2}{2} > 0$ is correct, meaning that the correct root $\boldsymbol{\omega}_{c1}$ can be obtained as follows:

$$\omega_{c1} = \sqrt{-\frac{a^2+b^2}{2} + \frac{1}{2}\sqrt{(a^2+b^2)^2 - 4(a^2b^2 - c^2d^2)}}$$

Therefore, t_{c1} can be expressed as follows:

$$t_{c1} = \frac{1}{\omega_{c1}}(\arccos\frac{\omega_{c1}^2+ab}{cd} + 2\pi j_1), \quad j_1 = 0, 1, \ldots$$

Defining $t_{j1} = t_{c1} + 2\pi j/\omega_{c1}$ ($j_1 = 0, 1, 2, \ldots$), then (t_{j1}, ω_{c1}) is the root of characteristic Equation (9).

(b) Similarly, assuming that $\omega\boldsymbol{i}$ (including $\omega > 0$) is a root of characteristic Equation (10), when the characteristic root $\omega\boldsymbol{i}$ is substituted in characteristic Equation (10), it can be expressed by Formula (17).

$$-\omega^2 + [b - a(1 - 2u_0)]\omega\boldsymbol{i} + c(d - 2u_0)(\cos\omega t_0 - \boldsymbol{i}\sin\omega t_0) - a(1 - 2u_0)b = 0 \tag{17}$$

The real part and imaginary part of Formula (17) can be separated as Formulas (18) and (19).

$$-\omega^2 - a(1 - 2u_0)b + c(d - 2u_0)\cos\omega t_0 = 0 \tag{18}$$

$$[b - a(1 - 2u_0)]\omega - c(d - 2u_0)\sin\omega t_0 = 0 \tag{19}$$

Because $\cos^2\omega t_0 + \sin^2\omega t_0 = 1$, Formulas (18) and (19) can then be reformulated as follows:

$$\omega^4 + [a^2(1 - 2u_0)^2 + b^2]\omega^2 + a^2(1 - 2u_0)^2b^2 - c^2(d - 2u_0)^2 = 0 \tag{20}$$

The root $\omega^2 < 0$ for Formula (20) should be rejected according to the practical meaning, then:

$$\omega^2 = -\frac{a^2(1 - 2u_0)^2 + b^2}{2} + \frac{1}{2}\sqrt{[a^2(1 - 2u_0)^2 + b^2]^2 - 4[a^2(1 - 2u_0)^2b^2 - c^2(d - 2u_0)^2]} \tag{21}$$

Obviously, if Formula (21) is correct, then an inequality such as $\frac{1}{2}\sqrt{[a^2(1 - 2u_0)^2 + b^2]^2 - 4[a^2(1 - 2u_0)^2b^2 - c^2(d - 2u_0)^2]} - \frac{a^2(1-2u_0)^2+b^2}{2} > 0$ is also cor-

rect. Therefore, the proof problem of Formula (21) can be transformed as the proof problem of Formula (22).

$$[a^2(1-2u_0)^2+b^2]^2-4[a^2(1-2u_0)^2b^2-c^2(d-2u_0)^2]>[a^2(1-2u_0)^2+b^2]^2 \quad (22)$$

After Formula (22) is reformulated, it is equivalent to Formula (23).

$$c^2(d-2u_0)^2>a^2(1-2u_0)^2b^2 \quad (23)$$

Based on known conditions such as $(a+b)^2/(4c)<d<1$, then inequalities such as $2cd>c+ab$ and $2u_0>1$ are concluded; therefore, Formula (23) is equivalent to $c(2u_0-d)>ab(2u_0-1)$, meaning that an inequality such as $c(2u_0-d)>ab(2u_0-1)$ is equivalent to an inequality such as $cd-ab>0$. Therefore, an inequality such as $\frac{1}{2}\sqrt{[a^2(1-2u_0)^2+b^2]^2-4[a^2(1-2u_0)^2b^2-c^2(d-2u_0)^2]}-\frac{a^2(1-2u_0)^2+b^2}{2}>0$ is correct, meaning that the correct root ω_{c2} can be obtained as follows:

$$\omega_{c2}=\sqrt{-\frac{a^2(1-2u_0)^2+b^2}{2}+\frac{1}{2}\sqrt{[a^2(1-2u_0)^2+b^2]^2-4[a^2(1-2u_0)^2b^2-c^2(d-2u_0)^2]}}$$

Then t_{c2} can be expressed by Formula (24):

$$t_{c2}=\frac{1}{\omega_{c2}}[\arccos\frac{\omega_{c2}^2+a(1-2u_0)b}{c(d-2u_0)}+2\pi j_2],\quad j_2=0,1,\ldots \quad (24)$$

Defining $t_{j2}=t_{c2}+2\pi j/\omega_{c2}(j_2=0,1,2,\ldots)$, then (t_{j2},ω_{c2}) is the root of characteristic Equation (10).

The proof of Theorem 1 is complete. □

Theorem 2. *Supposing that $\lambda(t_0)=r(t_0)+i\omega(t_0)$ is the characteristic root of characteristic Equation (9) and characteristic Equation (10) meets $r(t_{j1})=0$, $\omega(t_{j1})=\omega_{c1}(j_1=0,1,\ldots)$, $r(t_{j2})=0$, and $\omega(t_{j2})=\omega_{c2}(j_2=0,1,\ldots)$, then the following conclusions can be made: (a) For the real part of the characteristic root of characteristic Equation (9) in t_{j1}, its derivative $dr(t_0)/dt_0$ is positive; (b) When inequalities such as $2cd>c+ab$ are correct, and for the real part of the characteristic root of characteristic Equation (10) in t_{j2}, its derivative $dr(t_0)/dt_0$ is positive.*

Proof.

(a) Simultaneous derivations on both sides of characteristic Equation (9) are calculated based on variable t_0, and it can be expressed as follows:

$$2\lambda(t_0)\frac{\mathrm{d}\lambda(t_0)}{\mathrm{d}t_0}+(b-a)\frac{\mathrm{d}\lambda(t_0)}{\mathrm{d}t_0}-cdt_0\mathrm{e}^{-t_0\lambda(t_0)}\frac{\mathrm{d}\lambda(t_0)}{\mathrm{d}t_0}-cd\lambda(t_0)\mathrm{e}^{-t_0\lambda(t_0)}=0 \quad (25)$$

After Formula (25) is rearranged, Formula (26) is obtained.

$$\frac{\mathrm{d}\lambda(t_0)}{\mathrm{d}t_0}=\frac{cd\lambda(t_0)\mathrm{e}^{-t_0\lambda(t_0)}}{2\lambda(t_0)+(b-a)-cdt_0\mathrm{e}^{-t_0\lambda(t_0)}} \quad (26)$$

After $\lambda(t_0)=r(t_0)+iw(t_0)$ is put into Formula (26), Formula (27) is obtained.

$$\frac{\mathrm{d}[\mathrm{Re}\,\lambda(t_0)]}{\mathrm{d}t_0}\Big|_{t_0=t_{j1}}^{\lambda(t_{j1})=i\omega_{c1}}=\frac{\omega_{c1}^2(2\omega_{c1}^2+a^2+b^2)}{[b-a-t_{j1}\omega_{c1}^2-t_{j1}ab]^2+[2\omega_{c1}+(b-a)t_{j1}\omega_{c1}]^2}>0 \quad (27)$$

(b) When inequalities such as $2cd>c+ab$ are correct, the derivative $\mathrm{d}r(t_0)/\mathrm{d}t_0$ of the real part of the characteristic root of characteristic Equation (10) in t_{j2} is positive and Formula (28) is obtained.

$$\frac{\mathrm{d}[\mathrm{Re}\,\lambda(t_0)]}{\mathrm{d}t_0}\Big|_{t_0=t_{j2}}^{\lambda(t_{j2})=i\omega_{c2}} = \frac{\omega_{c2}^2[2\omega_{c2}^2 + a^2(1-2u_0)^2 + b^2]}{[b-a+2au_0 - t_{j2}\omega_{c2}^2 - t_{j2}a(1-2u_0)b]^2 + [2\omega_{c2} + (b-a+2au_0)t_{j2}\omega_{c2}]^2} > 0 \quad (28)$$

Based on Theorem 1, it can be concluded that characteristic Equation (9) in the balance point E_1 can produce Hopf bifurcation when $t_0 = t_{c1}$ and characteristic Equation (10) in the balance point E_2 can produce Hopf bifurcation when $t_0 = t_{c2}$.

The proof of Theorem 2 is complete. □

Theorem 3.

(a) If b is greater than a and t_0 belongs to closed interval [0, t_{c1}], then all characteristic roots of characteristic Equation (9) are of strictly negative real parts and E_1 is asymptotically stable.

(b) If b is greater than a and t_0 is greater than t_{c1}, then at least one characteristic root of characteristic Equation (9) is of a positive real part and E_1 is not stable.

(c) If b is not greater than a, then E_1 will be not stable when t_0 is greater than 0.

Proof.

(a) When t_0 is equal to 0, characteristic Equation (9) can be changed into $\lambda^2 + (b - \mathrm{a})\lambda - ab + cd = 0$. Given that b is greater than a, then all characteristic roots of the new characteristic equation such as $\lambda^2 + (b - \mathrm{a})\lambda - ab + cd = 0$ are of strictly negative real part. That is, the multiplicity sum of the root which is located in the right half-plane is zero. When t_0 belongs to closed interval [0, t_{c1}], characteristic Equation (9) is not of pure virtual root and zero root, and the zero points located in the right half-plane for the characteristic equation are uniformly bounded (when $|\lambda| \geq N$ (N is a positive number), $\lambda^2 + (b-a)\lambda - ab + cd\exp(-\lambda t_0) = 0$, and $|\lambda| = [(b-a)\lambda - ab + cd\exp(-\lambda t_0)]/|\lambda| \leq N_0$ (N_0 is a positive number)); therefore, all characteristic roots of characteristic Equation (9) are of strictly negative real parts when t_0 belongs to closed interval [0, t_{c1}] and E_1 is asymptotically stable.

(b) If b is greater than a and t_0 is greater than t_{c1}, then, according to Theorem 2, it is known that at least one characteristic root of characteristic Equation (9) is of a positive real part and E_1 is not stable.

(c) If b is not greater than a, when t_0 is greater than 0, making $f(\lambda) = \lambda^2 + (b-a)\lambda - ab + cd\exp(-\lambda t_0)$ and $\lambda = \alpha + \omega i$, then the imaginary part of $f(\lambda)$ can be expressed as follows:

$$2\alpha\omega + (b-a)\omega - cd\,\exp(-\alpha t_0)\sin\omega t_0 = 0$$

Given that the imaginary part of the equation $f(\lambda)$ is an odd function about parameter ω, then only the situations that ω is greater than or equal to 0 need be considered.

(1) If ω is greater than 0, then α will be greater than 0.

Proving the reverse is useful for solving the problem. Assuming that a is not greater than 0 and t_0 is greater than 0, the function $\sin\omega_{t0}$ can be expanded by Taylor's formula as follows:

$$\begin{aligned}
\alpha &= [cd\exp(-\alpha t_0)\sin\omega t_0 - (b-a)\omega]/2\omega \\
&= \omega[cdt_0\exp(-\alpha t_0)(\sin\omega t_0)/\omega t_0 + (a-b)]/2\omega \\
&= [cdt_0\exp(-\alpha t_0)\{\{[\omega t_0 - (\omega t_0)^3/3! + (\omega t_0)^5/5! - (\omega t_0)^7/7! + \dots\,]/\omega t_0\} + (a-b)\}/2 \\
&= [cdt_0\exp(-\alpha t_0)\{[1 - (\omega t_0)^2/3! + (\omega t_0)^4/5! - (\omega t_0)^6/7! + \dots\,] + (a-b)\}/2 > 0
\end{aligned}$$

Reversing the above proves the result and the assumption is contradictory; therefore, $\mathrm{Re}\lambda = \alpha$ is certainly greater than 0.

(2) If ω is equal to 0, then α will be greater than 0.

Only the real roots of $f(\lambda) = 0$ are considered. Obviously, $\lambda = 0$ is not the real root of $f(\lambda) = 0$ because $f(0) = cd - ab > 0$.

Assuming that equation $f(\lambda) = 0$ is of a real root, then λ will be greater than 0.

Proving the reverse is useful for solving the problem. Assuming that λ is less than 0, for an inequality such as $t_0 > 0$, the characteristic root of the equation $f(\lambda) = 0$ can be expressed as $\lambda^2 + (b - a)\lambda - ab + cd\exp(-\lambda t_0) = 0 > \lambda^2 + (b - a)\lambda - ab + cd$. In addition, an inequality such as $\lambda^2 + (b - a)\lambda - ab + cd > 0$ is known, so reversing the above proves the result and the assumption is contradictory; therefore, λ must be greater than 0 when the equation $f(\lambda) = 0$ is of a real root.

Therefore, if b is not greater than a, then E_1 is not stable when t_0 is greater than 0.

The proof of Theorem 3 is complete. □

Theorem 4. *If $2cd > c + ab$, $ab + bc > c + a^2b$, then E_2 is unstable when t_0 is greater than 0.*

Proof. Make $f(\lambda) = \lambda^2 + [b - a(1 - 2u_0)]\lambda - ab(1 - 2u_0) + c(d - 2u_0)\exp(-\lambda t_0)$; moreover, assuming that equations such as $p = b - a(1 - 2u_0)$, $s = -ab(1 - 2u_0)$, $q = c(d - 2u_0)$ and $\lambda = \alpha + \omega i$ are established, equations such as $f(\lambda) = \lambda^2 + p\lambda + s + q\exp(-\lambda t_0)$ can be easily derived.

Therefore, the imaginary part of the equation $f(\lambda)$ is expressed as follows:

$$2\alpha\omega + p\omega - q\exp(-\alpha t_0)\sin\omega t_0 = 0$$

Given that the imaginary part of the equation $f(\lambda)$ is an odd function about ω, then only the situation that ω is not less than 0 must be considered.

(1) If ω is greater than 0, then α will be greater than 0.

Proving the reverse is useful for solving the problem. Assuming that a is not greater than 0 and t_0 is greater than 0, then the Taylor expanded formula of $\sin\omega_{t0}$ can be expressed as follows:

$$\begin{aligned}
&\alpha = [q\exp(-\alpha t_0)\sin\omega t_0 - p\omega]/2\omega\\
&=\omega[qt_0\exp(-\alpha t_0)(\sin\omega t_0)/\omega t_0 - p]/2\omega\\
&=[qt_0\exp(-\alpha t_0)\{\{[\omega t_0 - (\omega t_0)^3/3! + (\omega t_0)^5/5! - (\omega t_0)^7/7! + \dots\ ]/\omega t_0\} - p\}/2\\
&=[qt_0\exp(-\alpha t_0)\{[1 - (\omega t_0)^2/3! + (\omega t_0)^4/5! - (\omega t_0)^6/7! + \dots\ ] - p\}/2
\end{aligned}$$

An inequality such as $q < 0$ can be concluded based on an inequality such as $2cd > c + ab$; moreover, an inequality such as $p > 1$ can also be concluded based on an inequality such as $ab + bc > c + a^2$; therefore, the following inequality can also be concluded:

$$\alpha = [qt_0\exp(-\alpha t_0)\{[1 - (\omega t_0)^2/3! + (\omega t_0)^4/5! - (\omega t_0)^6/7! + \dots\ ] - p\}/2 > 0$$

Obviously, reversing the above proves the result and the assumption is contradictory; therefore, an inequality such as $\mathrm{Re}\lambda = \alpha > 0$ is correct.

(2) If ω is equal to 0, then α will be greater than 0.

Because $\lambda = 0$ is not the real root of the characteristic equation $f(\lambda) = 0$, only the real roots of the characteristic equation $f(\lambda) = 0$ are considered.

Consider that the characteristic equation $f(0) = q + s = c(d - 2u_0) - ab(1 - 2u_0) = cd - ab + 2u_0(ab - c) = cd - ab + 2(ab - c)\cdot(ab - cd)/(ab - c) = ab - cd$ is less than 0 when λ is equal to 0. In addition, assuming that the characteristic equation $f(\lambda) = 0$ is of the real root, then λ will be greater than 0.

Proving the reverse is used to solve the problem. Assuming that λ is less than 0 when t_0 is greater than 0, then the characteristic root of the characteristic equation $f(\lambda) = 0$ is concluded as an inequality such as $\lambda^2 + p\lambda + s+q\exp(-\lambda t_0) = 0 < \lambda^2 + p\lambda + s+q$. When the characteristic root λ is less than 0, two inequalities such as $\lambda^2 + p\lambda + s+q < 0$ and $\lambda^2 + p\lambda + s+q > 0$ and an equality such as $\lambda^2 + p\lambda + s+q = 0$ are correct. Therefore, the hypothesis is incorrect; that is, when the characteristic equation $f(\lambda) = 0$ is of a real root, then λ must be greater than 0.

Therefore, if two inequalities such as $2cd > c + ab$ and $ab + bc > c + a^2b$ are correct, then E_2 is not stable when t_0 is greater than 0.

The proof of Theorem 4 is complete. □

3.3. Analysis of the Nonlinear Dynamic Evolution of Human–Machine Safety System under a Low Carbon Manufacturing Process

According to the established nonlinear dynamic evolution mathematical model of human–machine safety system with large time delay under a low carbon manufacturing process, the interactive evolution model between alertness and safety can be analyzed qualitatively through the phase diagram analysis, with the analysis results providing a basis for the safety assessment and control.

According to Theorems 1–4, the phase diagrams as Figures 1–3 of the nonlinear dynamic evolution for the human–machine safety system with large time delay under a low carbon manufacturing process can be drawn out.

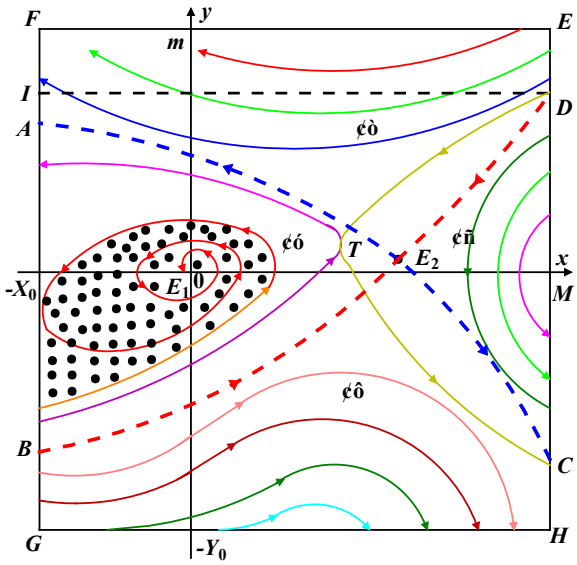

Figure 1. Asymptotically stable situation of the odd point $E_1(0, 0)$.

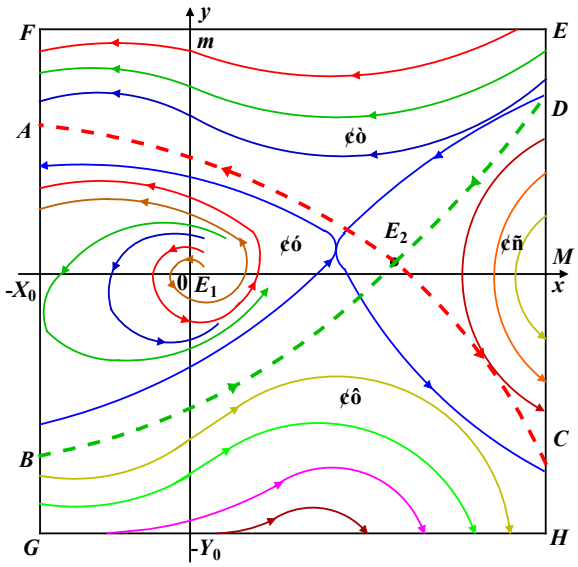

Figure 2. Unstable situation of the odd point $E_1(0, 0)$.

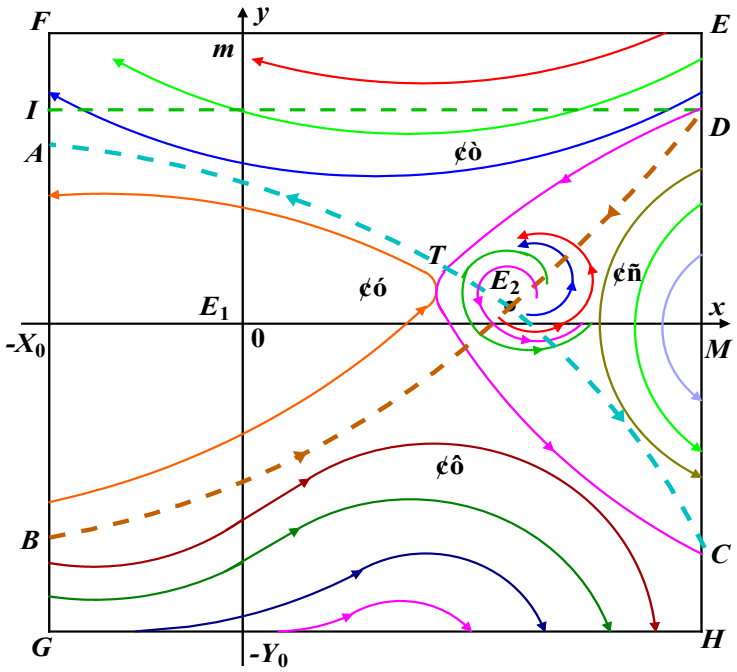

Figure 3. Unstable situation of the odd point $E_2(u_0, v_0)$.

As shown in Figure 1, the curved trapezoid *DBGHD* is the development area of the human–machine safety system with large time delay under a low carbon manufacturing process, the shaded part area is the instability area of the man–machine safety system with large time delay under low carbon manufacturing process, and the rest area is the collapse area of the human–machine safety system with large time delay under a low carbon manufacturing process. Moreover, the *EFGH* area can also be divided into four dynamic areas: the safety area I, the deterioration area II, the asymptotically stable safety area III, and the enhancement area IV of the safety ability.

(1) Asymptotically stable situation of the odd point E_1 (0, 0)

Based on the dynamic evolution model of the man–machine safety system with large time delay, formulas such as $a = a_1/a_2$ and $b = b_2/a_2$ can be concluded.

When b is greater than a and t_0 belongs to closed interval $[0, t_{c1}]$ is correct, it means that a_1 is less than b_2 and τ_0 belongs to closed interval $[0, \tau_{c1}/a_2]$ is also correct. Given that the equivalent time delay τ_0/a_2 and the safety level intrinsic growth a_1 of the man–machine safety system with large time delay under a low carbon manufacturing process is less than the comprehensive effects of the carelessness resistance coefficient b_2, then the dynamic evolution model of the man–machine safety system with large time delay under a low carbon manufacturing process is of two singularities, such as $E_1(0, 0)$ and $E_2(u_0, v_0)$. As shown in Figure 1, $E_1(0, 0)$ is an asymptotically stable point without a closed rail.

When τ_0 belongs to closed interval $[0, \tau_{c1}/a_2]$, based on the phase diagram analysis from Figure 1, some qualitative analysis results about the nonlinear dynamic evolution of the man–machine safety system with large time delay under a low carbon manufacturing process can be obtained as follows:

(a) In area I: The carelessness level of the man–machine safety system with large time delay is relatively low, the influence of equivalent time delay τ_0/a_2 is small, and the safety level of the man–machine safety system with large time delay is quite stable; therefore, the safety development trend is very good.

(b) In area II: The influence of equivalent time delay τ_0/a_2 is still not big, but the carelessness level of the man–machine safety system with large time delay is increasingly higher, while the safety level of the man–machine safety system will

deteriorate continuously, eventually causing the man–machine safety system to collapse.

(c) In area III: The influence of the equivalent time delay is not big, and the man–machine safety system with large time delay is in a weakened oscillation state; therefore, the oscillation amplitudes of the carelessness level and the safety level are also weakened and they ultimately tend to the balance point $E_1(0, 0)$.

(d) In area IV: The influence of equivalent time delay τ_0/a_2 is not big, and the intrinsic growth a_1 of the safety level is less than the comprehensive function of the carelessness resistance coefficient b_2, which will continuously improve the safety capacity of the man–machine safety system with large time delay. Finally, the safety level can be closed to the threshold value M of the man–machine safety system with large time delay.

(2) Unstable situation of the odd point $E_1(0, 0)$

Based on the dynamic evolution model of the human–machine safety system, if b is greater than a and t_0 is greater than t_{c1}, it means that a_1 is less than b_2 and τ_0 is greater than τ_{c1}/a_2. Therefore, it can be concluded that the intrinsic growth a_1 of the safety level of the man–machine safety system is less than the carelessness resistance coefficient b_2 due to the influence of the larger equivalent time delay τ_{c1}/a_2, while the singular point $E_1(0, 0)$ in the dynamic evolution model of the man–machine safety is an unstable point. As shown in Figure 2, when b is not greater than a and t_0 is greater than 0 (namely b_2 is less than a_1 and τ_0 is greater than 0), the intrinsic growth a_1 of the safety level is greater than the carelessness resistance coefficient b_2 and the singularity $E_1(0, 0)$ is an unstable point as long as there is an effect from the equivalent time delay.

Based on the compared results between Figures 1 and 2, it is known that area I, area II, and area IV have basically the same evolution patterns, but area III is in a different evolution state. The main reasons are: due to the influence of larger equivalent time delay τ_{c1}/a_2, when the intrinsic growth a_1 of the safety level of the man–machine safety system is less than the carelessness resistance coefficient b_2 or the intrinsic growth a_1 of the safety level is greater than the carelessness resistance coefficient b_2, the intrinsic growth rate of the safety level of the man–machine safety system is greatly suppressed and the carelessness level is greatly enhanced, which can lead to the small degree divergent oscillation of the safety level and carelessness level in the areas (for example, the singular point $E_1(0, 0)$ is an unstable focus). With the passing of time, the safety level of the man–machine safety system will eventually tend to collapse after a certain divergent oscillation.

(3) Unstable situation of the odd point $E_2(u_0, v_0)$

Based on the dynamic evolution model of the man–machine safety system, if $2cd$ is greater than $c + ab$, $ab + bc$ is greater than $c + a^2b$, and t_0 is greater than 0 (namely $2a_2b_1m$ is greater than $a_2b_1M + a_1b_2$, $a_1a_2b_2 + a_2b_1b_2M$ is greater than $b_1{a_2}^2M + b_2{a_1}^2$, and τ_0 is greater than 0), then the difference between the intrinsic growth b_1 of the carelessness level and the intrinsic growth rate a_1 of the safety level, respectively, may consist of three kinds of spiral oscillations, namely the difference $b_1 - a_1$ may be greater than zero, the difference $b_1 - a_1$ may be equal to zero, or the difference $b_1 - a_1$ may be less than zero, while the coefficient a_2 for the effect of the carelessness on safety and the carelessness resistance coefficient b_2 are basically equal. As shown in Figure 3, the dynamic evolution model of the human–machine safety system has another unstable point $E_2(u_0, v_0)$, but it is not of a limit ring. Moreover, the intrinsic growth rate a_1 of the safety level (or the intrinsic growth rate b_1 of the carelessness level) is of a large degree spiral oscillation suppression, which will lead to divergent oscillation (such as singular point $E_2(u_0, v_0)$ for an unstable point) in area I, area II, area III, and area IV. With the passing of time, the safety level of the man–machine safety system will also eventually tend to collapse after a certain divergent oscillation.

3.4. Qualitative Analysis of the Nonlinear Dynamic Evolution Trend of the Human–Machine Safety System

As shown in Figure 4, due to the nonlinear dynamic evolution phase diagram of the human–machine safety system, the nonlinear dynamic evolution trend of the man–machine safety system can also be qualitatively analyzed.

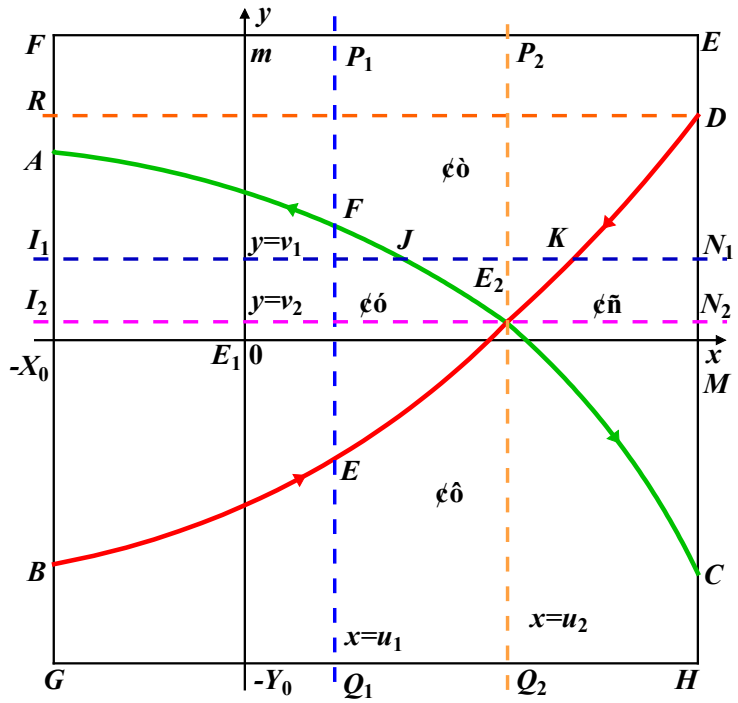

Figure 4. Qualitative analysis of nonlinear dynamic evolution trend on the human–machine safety.

(1) When the safety level is a fixed value

Figure 4 shows that when the safety level of the man–machine safety system is $x = u_1$ and the line $x = u_1$ is of two intersection points E and F in the phase diagram with the curve AC and the curve BD, there are three possibilities for the corresponding safety areas, namely the line segments EF, FP_1, and EQ_1 represent the safety oscillation area, the safety deterioration area, and the safety enhancement area, respectively.

When line $x = u_1$ moves to the right, the safety oscillation area will decrease, while the safety enhancement area and the safety deterioration area will increase. When line $x = u_1$ moves to the left, the safety oscillation area will increase, while the safety enhancement area and the safety deterioration area will decrease. Given that the line $x = u_2$ is of one intersection point $E_2(u_0, v_0)$ in the phase diagram with the curve AC and the curve BD, there are therefore two possibilities for the corresponding safety area, namely the line segments E_2P_1 and E_2Q_1 represent the safety deterioration area and the safety enhancement area, respectively.

When the deterioration degree of the carelessness level is still under the line DR, if the carelessness level is no longer increased, then the state of the safety level can be returned to the development area of the human–machine safety system as long as the operation level and rapid strain ability need to be improved.

(2) When the carelessness level is a fixed value

Figure 4 shows that when the carelessness level of the human–machine safety system is $y = v_1$ and the line $y = v_1$ is of two intersection points J and K in the phase diagram with the curve AC and the curve BD, there are three possibilities for the corresponding safety areas, namely the line segments I_1J, JK, and KN_1 represent the safety oscillation area, the safety deterioration area, and the safety enhancement area, respectively.

When the carelessness level decreases, the line $y = v_1$ will move down and the safety deterioration area will decrease, but the safety oscillation area and the safety area will increase; therefore, the possibility of safety deterioration will also decrease. Given that the line $y = v_2$ is of one intersection point $E_2(u_0,v_0)$ in the phase diagram with the curve AC and the curve BD, there are therefore two possibilities for the corresponding safety area, namely the line segments E_2I_2 and E_2N_2 represent the safety oscillation area and the safety enhancement area, respectively.

When the safety state of the man–machine safety system is beyond the development area of the man–machine safety system, if the operation level and rapid strain ability is no longer increased, then the state of the safety level can be returned to the development area of the human–machine safety system as long as the carelessness level can be overcome.

4. Empirical Analysis

4.1. Low Carbon Level Evaluation of Human–Machine Safety System under a Low Carbon Manufacturing Process

The technological process of radial tire casing can be expressed as Figure 5.

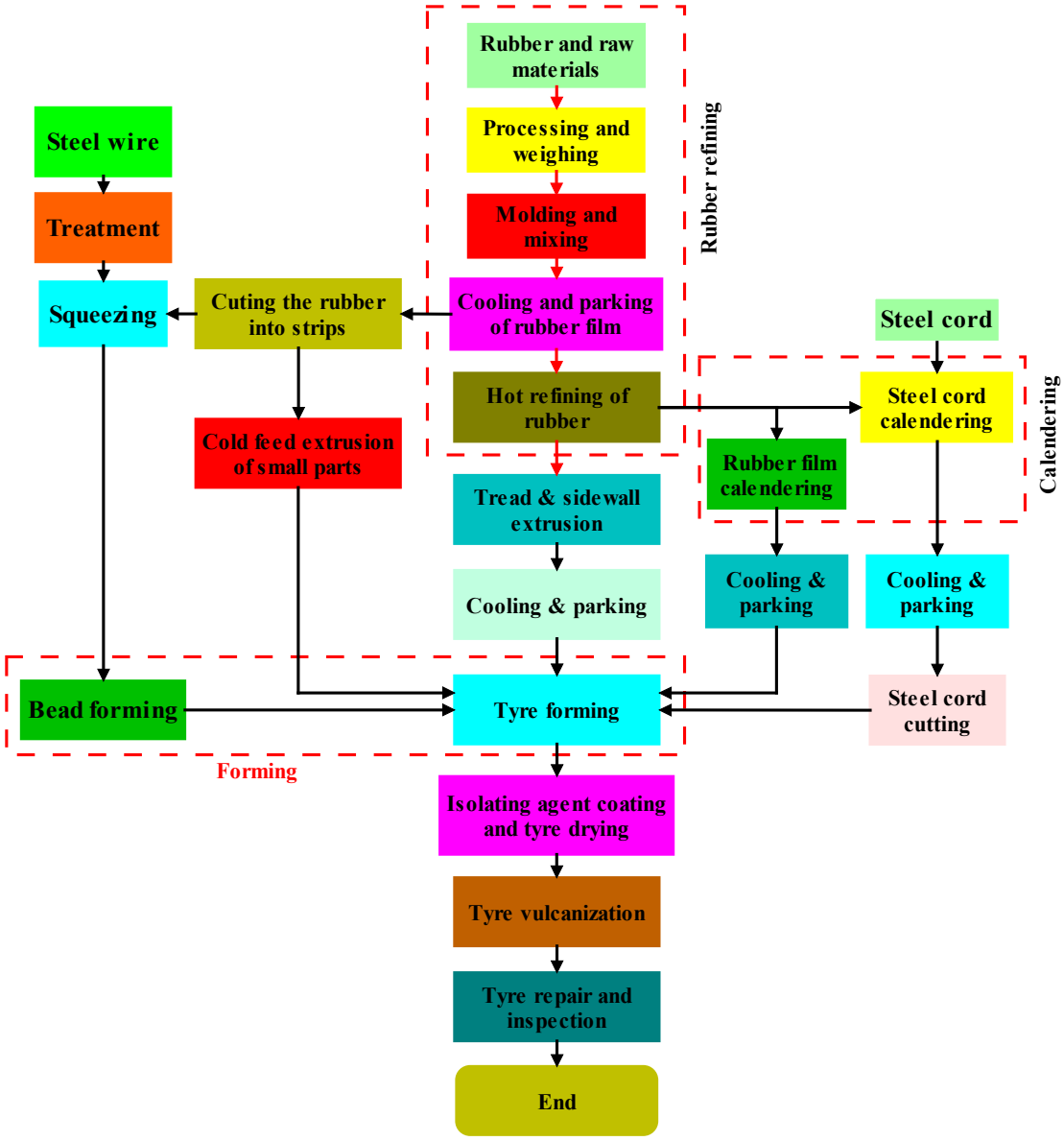

Figure 5. Technological process of radial tire casing.

According to the evaluation system shown in Figure 5, the low carbon level evaluation value C_L of the radial tire casing process mainly includes three aspects: low carbon structure, low carbon technology, and low carbon management.

The evaluation value C_{L1} of the low carbon structure includes: raw rubber grade C_{L11}, proportion C_{L12} of electric energy consumption, and degree C_{L13} of automation.

The evaluation value C_{L2} of the low carbon technology includes: unit consumption C_{L21} of tire manufacturing, recovery rate C_{L22} of waste rubber, and operation rate C_{L23}.

The evaluation value C_{L2} of the low carbon management includes: labor productivity C_{L31}, allocation rate C_{L32} of measuring instruments, and energy management level C_{L33}.

The selection of the number of evaluation criteria should be appropriate. In general, choose t = 5; that is, the rating mode is set as excellent, good, medium, poor, and worse. Therefore, the evaluation scale set for low carbon level of the radial tire casing process can be expressed as:

$$V = (v_1, v_2, v_3, v_4, v_5) \tag{29}$$

where v_1, v_2, v_3, v_4, and v_5 represents the rating mode of excellent, good, medium, poor, and worse, respectively, and V = (0.9, 0.7, 0.5, 0.3, 0.1).

When calculating the membership degree of each index, the method of "ideal value proximity" is used in combination with expert scoring. The ideal value is the highest or lowest value of each index (the benefit index and the cost index are the highest value and the lowest value, respectively). Combined with the relevant data of radial tire casing manufacturing, the calculated membership degree of each index relative to the evaluation scale set is shown in Table 1.

Table 1. Membership degree of each index relative to evaluation scale set $\boldsymbol{V}$.

Index	Membership Degree				
	Excellent	**Good**	**Medium**	**Poor**	**Worse**
C_{L11}	0.66	0.13	0.07	0.10	0.04
C_{L12}	0.26	0.11	0.26	0.23	0.14
C_{L13}	0.48	0.23	0.13	0.10	0.06
C_{L21}	0.52	0.27	0.11	0.07	0.03
C_{L22}	0.71	0.16	0.10	0.03	0.00
C_{L23}	0.64	0.19	0.07	0.03	0.07
C_{L31}	0.44	0.17	0.22	0.10	0.07
C_{L32}	0.36	0.26	0.10	0.14	0.14
C_{L33}	0.39	0.30	0.13	0.08	0.10

According to the membership degree of the influencing factors relative to the evaluation scale set V shown in Table 1, the single factor fuzzy relationship matrix of each influencing factor relative to the corresponding evaluation index can be calculated as follows:

$$\boldsymbol{E}_1 = \begin{bmatrix} 0.66 & 0.13 & 0.07 & 0.10 & 0.04 \\ 0.26 & 0.11 & 0.26 & 0.23 & 0.14 \\ 0.48 & 0.23 & 0.13 & 0.10 & 0.06 \end{bmatrix}$$

$$\boldsymbol{E}_2 = \begin{bmatrix} 0.52 & 0.27 & 0.11 & 0.07 & 0.03 \\ 0.71 & 0.16 & 0.10 & 0.03 & 0 \\ 0.64 & 0.19 & 0.07 & 0.03 & 0.07 \end{bmatrix}$$

$$\boldsymbol{B} = \begin{bmatrix} \boldsymbol{C}_1 \\ \boldsymbol{C}_2 \\ \boldsymbol{C}_3 \end{bmatrix} = \begin{bmatrix} 0.5186\ 0.1886\ 0.1218\ 0.1107\ 0.0603 \\ 0.5768\ 0.2362\ 0.1040\ 0.0567\ 0.0262 \\ 0.3859\ 0.2763\ 0.1296\ 0.0994\ 0.1089 \end{bmatrix}$$

Based on the analytic hierarchy process, weight coefficient matrix W of the low carbon level evaluation value C_L, weight coefficient matrix W_1 of the low carbon level evaluation value C_{L1}, weight coefficient matrix W_2 of the low carbon level evaluation value C_{L2}, and

weight coefficient matrix W_3 of the low carbon level evaluation value C_{L3} can be calculated as: W = (0.2299, 0.6479, 0.1222), W_1 = (0.3151, 0.0824, 0.6025), W_2 = (0.6687, 0.2431, 0.0882), and W_3 = (0.0926, 0.2924, 0.6150), respectively.

Therefore, the single factor fuzzy relationship matrix of each influencing factor relative to the corresponding evaluation index can be calculated as follows:

$$\begin{aligned}\boldsymbol{C}_1 = \boldsymbol{W}_1 \times \boldsymbol{E}_1 &= \begin{bmatrix}0.3151 & 0.0824 & 0.6025\end{bmatrix}\begin{bmatrix}0.66 & 0.13 & 0.07 & 0.10 & 0.04\\ 0.26 & 0.11 & 0.26 & 0.23 & 0.14\\ 0.48 & 0.23 & 0.13 & 0.10 & 0.06\end{bmatrix}\\ &= (0.5186,\ 0.1886,\ 0.1218,\ 0.1107,\ 0.0603)\end{aligned}$$

$$\begin{aligned}\boldsymbol{C}_2 = \boldsymbol{W}_2 \times \boldsymbol{E}_2 &= \begin{bmatrix}0.6687 & 0.2431 & 0.0882\end{bmatrix}\begin{bmatrix}0.52 & 0.27 & 0.11 & 0.07 & 0.03\\ 0.71 & 0.16 & 0.10 & 0.03 & 0\\ 0.64 & 0.19 & 0.07 & 0.03 & 0.07\end{bmatrix}\\ &= (0.5768,\ 0.2362,\ 0.1040,\ 0.0567,\ 0.0262)\end{aligned}$$

$$\begin{aligned}\boldsymbol{C}_3 = \boldsymbol{W}_3 \times \boldsymbol{E}_3 &= \begin{bmatrix}0.0926 & 0.2924 & 0.6150\end{bmatrix}\begin{bmatrix}0.44 & 0.17 & 0.22 & 0.10 & 0.07\\ 0.36 & 0.26 & 0.10 & 0.14 & 0.14\\ 0.39 & 0.30 & 0.13 & 0.08 & 0.10\end{bmatrix}\\ &= (0.3859,\ 0.2763,\ 0.1296,\ 0.0994,\ 0.1089)\end{aligned}$$

The fuzzy evaluation matrix $\boldsymbol{B}$ of each influencing factor relative to the evaluation index can be obtained as follows:

$$\boldsymbol{B} = \begin{bmatrix}\boldsymbol{C}_1\\ \boldsymbol{C}_2\\ \boldsymbol{C}_3\end{bmatrix} = \begin{bmatrix}0.5186\ 0.1886\ 0.1218\ 0.1107\ 0.0603\\ 0.5768\ 0.2362\ 0.1040\ 0.0567\ 0.0262\\ 0.3859\ 0.2763\ 0.1296\ 0.0994\ 0.1089\end{bmatrix}$$

Thus, the single factor fuzzy relationship matrix $\boldsymbol{C}$ of each influencing factor relative to the evaluation index can be calculated as follows:

$$\begin{aligned}\boldsymbol{C} = \boldsymbol{Q} \times \boldsymbol{B} &= \begin{bmatrix}0.2299 & 0.6479 & 0.1222\end{bmatrix}\begin{bmatrix}0.5186\ 0.1886\ 0.1218\ 0.1107\ 0.0603\\ 0.5768\ 0.2362\ 0.1040\ 0.0567\ 0.0262\\ 0.3859\ 0.2763\ 0.1296\ 0.0994\ 0.1089\end{bmatrix}\\ &= (0.5401,\ 0.2302,\ 0.1112,\ 0.0744,\ 0.0442)\end{aligned}$$

According to the established evaluation scale set $\boldsymbol{V}$ = (V_1, V_2, V_3, V_4, V_5) = (0.9, 0.7, 0.5, 0.3, 0.1), the evaluation value G of the low carbon level in the technological process of radial tire casing can be calculated as follows:

$$\begin{aligned}G &= \boldsymbol{C} \times \boldsymbol{V}^{\mathrm{T}} = [0.5401\ 0.2302\ 0.1112\ 0.0744\ 0.0442]\begin{bmatrix}0.9 & 0.7 & 0.5 & 0.3 & 0.1\end{bmatrix}^{\mathrm{T}}\\ &= 0.7295\end{aligned}$$

Comparing the value of G = 0.7295 with $\boldsymbol{V}$ = (0.9, 0.7, 0.5, 0.3, 0.1), the evaluation result is good. It can be determined that the low carbon level in the technological process of radial tire casing is good.

Similarly, the low carbon level evaluation value G_1 of the low carbon structure, the low carbon level evaluation value G_2 of the low carbon technology, and the low carbon level evaluation value G_3 of the low carbon management in the technological process of radial tire casing can be calculated, respectively, as follows:

$$G_1 = \boldsymbol{C}_1 \times \boldsymbol{V}^{\mathrm{T}} = [0.5186\ 0.1886\ 0.1218\ 0.1107\ 0.0603]\begin{bmatrix}0.9 & 0.7 & 0.5 & 0.3 & 0.1\end{bmatrix}^{\mathrm{T}} = 0.6989$$

$$G_2 = \boldsymbol{C}_2 \times \boldsymbol{V}^{\mathrm{T}} = [0.5768\ 0.2362\ 0.1040\ 0.0567\ 0.0262]\begin{bmatrix}0.9 & 0.7 & 0.5 & 0.3 & 0.1\end{bmatrix}^{\mathrm{T}} = 0.7561$$

$$G_3 = \boldsymbol{C}_3 \times \boldsymbol{V}^{\mathrm{T}} = [0.3859\ 0.2763\ 0.1296\ 0.0994\ 0.1089]\begin{bmatrix}0.9 & 0.7 & 0.5 & 0.3 & 0.1\end{bmatrix}^{\mathrm{T}} = 0.6462$$

The calculated low carbon levels in the technological process of radial tire casing are shown in Table 2.

Table 2. Low carbon level evaluation values in the technological process of radial tire casing.

Item	Low Carbon Structure	Low Carbon Technology	Low Carbon Management	Radial Tire Casing Process
Evaluation value	0.6989	0.7561	0.6462	0.7295
Evaluation grade	Medium	Good	Medium	Good

It can be seen that the low carbon development trend of the technological process of radial tire casing is "good", while the overall evaluation grade is "good". Among them, the low carbon level in process technology is good, which promotes the improvement of the low carbon level of technological process of radial tire casing. However, low carbon structure and low carbon management have slightly lower low carbon levels, which need to be optimized in these links.

4.2. Application of the Dynamic Evolution Model of Human–Machine Safety System under a Low Carbon Manufacturing Process

During the past 10 years, low carbon manufacturing equipment have been largely used under a low carbon manufacturing process, with the development including large scale, automated, and intelligent production. It is well known that the overall level of enhancement of the human–machine safety systems under a low carbon manufacturing process is a practical method for improving production, reducing production costs, and improving the conditions of the manufacturing safety. Figure 6 shows that the man–machine safety system under a low carbon manufacturing process mainly includes a man–drilling subsystem, a man–squeezing steel wire subsystem, a man–tread squeezing subsystem, a man–forklift subsystem, a man–steel cord calendaring subsystem, a man–rubber cutting subsystem, a man–steel cord cutting subsystem, a man–isolating agent baking subsystem, and a man–radial tire curing subsystem. These operations from the human–machine system can also be divided into checking activities, starting and stopping activities, maintenance activities, driving operation activities, and mining operation activities.

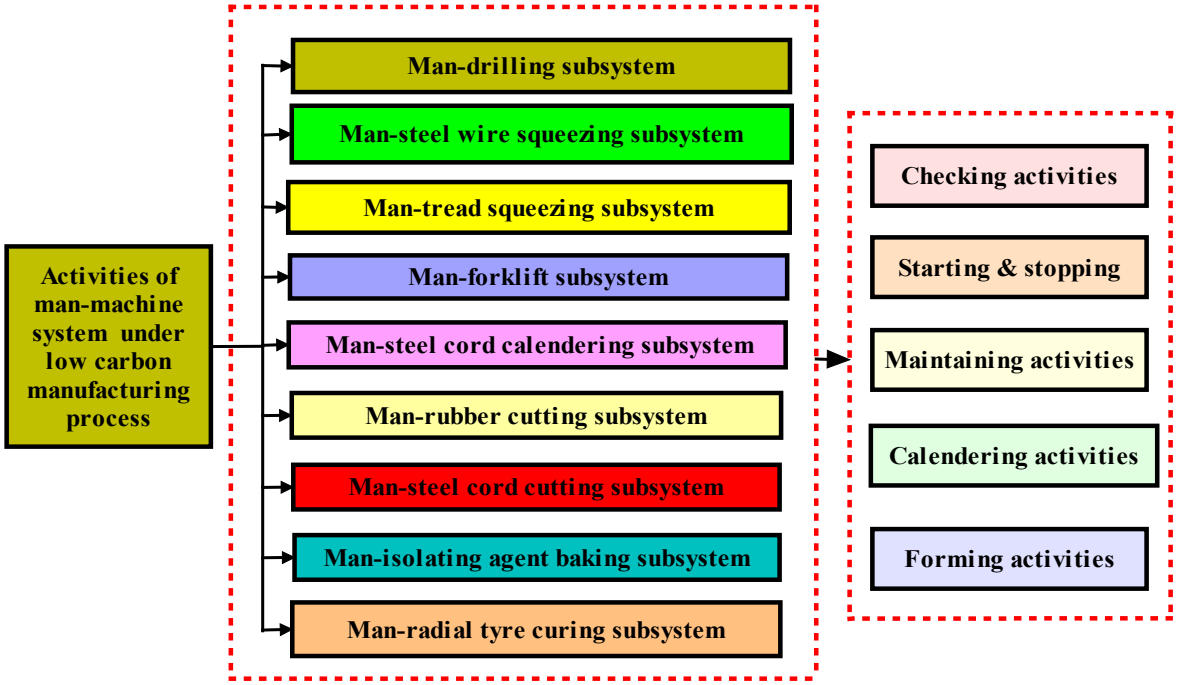

Figure 6. Man–machine safety system under a low carbon manufacturing process.

For different human–machine safety systems, their corresponding parameter set (a_1, a_2, b_1, b_2, m, M) is also different. Therefore, in order to investigate the nonlinear

dynamic evolution status ($x(\tau) = u$, $y(\tau) = v$) of the human–machine safety system under a low carbon manufacturing process, the parameter set (a_1, a_2, b_1, b_2, m, M) of the human–machine safety system under a low carbon manufacturing process must firstly be determined.

Let $x_1(\tau)$ = the safety level of the man–drill subsystem, $x_2(\tau)$ = the safety level of the man–squeezing steel wire subsystem, $x_3(\tau)$ = the safety level of the man–tread squeezing subsystem, $x_4(\tau)$ = the safety level of the man–forklift subsystem, $x_5(\tau)$ = the safety level of the man–steel cord calendaring subsystem, $x_6(\tau)$ = the safety level of the man–steel cord cutting subsystem, $x_7(\tau)$ = the safety level of the man–rubber cutting subsystem, $x_8(\tau)$ = the safety level of the man–isolating agent baking subsystem, and $x_9(\tau)$ = the safety level of the man–radial tire curing subsystem. Equation (30) can then be obtained.

$$x(\tau) = \sum_{i=1}^{9} \alpha_i x_i(\tau) \tag{30}$$

where α_i is the weight coefficient of the ith safety level.

Similarly, let $y_1(\tau)$ = the carelessness level of the man–drill subsystem, $y_2(\tau)$ = the carelessness level of the man–squeezing steel wire subsystem, $y_3(\tau)$ = the carelessness level of the man–tread squeezing subsystem, $y_4(\tau)$ = the carelessness level of the man–forklift subsystem, $y_5(\tau)$ = the carelessness level of the man–steel cord calendaring subsystem, $y_6(\tau)$ = the carelessness level of the man–steel cord cutting subsystem, $y_7(\tau)$ = the carelessness level of the man–rubber cutting subsystem, $y_8(\tau)$ = the carelessness level of the man–isolating agent baking subsystem, and $y_9(\tau)$ = the carelessness level of the man–radial tire curing subsystem. Equation (31) can then be obtained.

$$y(\tau) = \sum_{i=1}^{9} \beta_i y_i(\tau) \tag{31}$$

where β_i is the weight coefficient of the ith carelessness level.

Defining time delay as time interval, the ith safety level value $x_i(\tau)$ and the ith carelessness level value $y_i(\tau)$ in history can be determined by using a questionnaire survey and the expert evaluation method. Moreover, the analytic hierarchy method [31] is used to determine the weight coefficient α_i of the ith safety level and the weight coefficient β_i of the ith carelessness level.

Defining time delay as the time interval, the delay difference equations about Formulas (1) and (2) can be expressed as follows:

$$\frac{x(\tau) - x(\tau - \tau_0)}{\tau_0} = a_1 \cdot x(\tau)[1 - \frac{x(\tau)}{M}] - a_2 \cdot y(\tau - \tau_0) \tag{32}$$

$$\frac{y(\tau) - y(\tau - \tau_0)}{\tau_0} = b_1 \cdot x(\tau)[m - x(\tau)] - b_2 \cdot y(\tau) \tag{33}$$

After the obtained historical level values ($x(\tau)$ and $y(\tau)$) are substituted into Formulas (32) and (33), the corresponding parameter set (a_1, a_2, b_1, b_2, m, M) of the human–computer safety system under a low carbon manufacturing process can be obtained.

According to above method, the parameter set (a_1, a_2, b_1, b_2, m, M) = (0.20, 0.20, 0.7, 0.4, 0.80, 1.00) of the man–machine safety system under a low carbon manufacturing process can be obtained; therefore, results such as $a = a_1/a_2 = 1.0$, $b = b_2/a_2 = 2.0$, $c = b_1M/a_2 = 3.5$, and $d = m/M = 0.8$ can be concluded. It is obvious that inequalities such as $2cd > c + ab$ and $cd > ab$ are correct, while the equilibrium points of the human–machine safety system under a low carbon manufacturing process are $E_1 = (0, 0)$ and $E_2 = (0.5333, 0.2489)$.

Based on Theorem 1, results such as $\omega_{c1} = 0.8225$, $t_{c1} = 0.2981$, $\omega_{c2} = 0.4504$, and $t_{c2} = 2.3955$ can be obtained.

Based on Theorem 3 and calculated results such as $b = 2.0 > a = 1.0$ and $a_1 < b_2$, the stable states of the equilibrium points have two possibilities: (a) As shown in Figure 1, when t_0 belongs to closed interval $[0, t_{c1}]$, the changes in the carelessness level will affect

the development trend of the safety level and the equilibrium point E_1 is asymptotically stable; that is, with the passing of time, the carelessness phenomenon will tend to zero and the safety level will also tend to zero ($x = 0$); (b) As shown in Figure 2, when t_0 is greater than t_{c1}, the equilibrium point E_1 is not stable; that is, as time passes, changes in the carelessness level will have a serious block effect on safety development.

Based on Theorem 4 and calculated results such as $ab + bc - c - a^2b = 3.5 > 0$ (namely $ab + bc > c + a^2b$), the equilibrium point E_2 is not stable when t_0 is greater than 0; that is, with the passing of time, changes in the carelessness level will have a serious block effect on safety development, as shown in Figure 3.

The above results reveal that the established nonlinear dynamic evolution model of the human–machine safety system with large time delay under a low carbon manufacturing process can highlight the nonlinear dynamic evolution law of the human–machine safety system with large time delay.

5. Conclusions

(1) The dynamic evolution simulation results based on the mathematical analysis of the nonlinear dynamic evolution model demonstrate the validity and correctness of the nonlinear dynamic evolution model of the human–machine safety system.

(2) The qualitative analysis of the nonlinear dynamic evolution and the trend of the human–machine safety system with the large time delay reveals that there are four dynamic areas, namely the safety area I, the deterioration area II, the asymptotically stable safety area III, and the enhancement area IV of the safety ability based on the dynamic evolution model with large time delay between the carelessness level and the safety level.

(3) There are two singularities, $E_1(0, 0)$ and $E_2(u_0, v_0)$, in the dynamic evolution model of the man–machine safety system with large time delay under a low carbon manufacturing process. When the singularity $E_1(0, 0)$ is an asymptotically stable point and unstable point, respectively, area I, area II, and area IV have very similar evolution patterns, but area III has a different evolution state. In addition, another unstable point $E_2(u_0, v_0)$ can lead to divergent oscillation in area I, area II, area III, and area IV, where the safety level of the man–machine safety system with large time delay under a low carbon manufacturing process will eventually tend to collapse with time.

(4) For qualitative analysis of the nonlinear safety dynamic evolution trend, consider when the deterioration degree of the carelessness level is below the line DR in Figure 4. If the carelessness level no longer increases and the safety level is a fixed value, then the state of the safety level can be returned to the development area as long as the operation level and rapid strain ability is improved. When the safety state of the human–machine safety system is beyond the development area of the man–machine safety system, if the operation level and rapid strain ability are no longer increasing and the carelessness level is a fixed value, then the state of the safety level can be returned to the development area as long as the carelessness level can be overcome.

(5) Application case results of the radial tire casing process show that the overall evaluation grade of the low carbon development trend is "good". However, low carbon structure and management need to be optimized, and with the equilibrium points of the human–machine safety system under a low carbon manufacturing process being $E_1 = (0, 0)$ and $E_2 = (0.5333, 0.2489)$, changes in the carelessness level have a serious block effect on safety development over time.

Author Contributions: Conceptualization, B.L. and H.Z.; methodology, B.L. and H.Z.; software, B.L., Y.C. and G.J.; validation, B.L., Y.C., H.Z. and D.Z.; formal analysis, B.L., H.Z. and D.Z.; resources, B.L. and H.Z.; data curation, B.L., H.Z. and D.Z.; writing—original draft preparation, B.L., Y.C., H.Z. and D.Z.; writing—review and editing, B.L., Y.C., H.Z., G.J. and D.Z.; visualization, H.Z., G.J. and D.Z.; supervision, B.L. and H.Z.; project administration, B.L.; funding acquisition, B.L. and H.Z. All authors have read and agreed to the published version of the manuscript.

Funding: Project (52175135) supported by the Natural Science Foundation of China, Project (2022JJ50013) supported by the Natural Science Foundation of Hunan Province and Fund Project (202111342010) supported by the China Innovation Training Program for College Students.

Institutional Review Board Statement: Not applicable.

Informed Consent Statement: Not applicable.

Data Availability Statement: All data used to support the findings of this study are included within the article.

Acknowledgments: The authors would like to acknowledge Project (2022JJ50013) supported by the Natural Science Foundation of Hunan Province and Fund Project (202111342010) supported by the China Innovation Training Program for College Students.

Conflicts of Interest: The authors declare no conflict of interest.

References

1. Shojaeinasaba, A.; Charter, T.; Jalayer, M.; Khadivi, M.; Ogunfowora, O.; Raiyani, N.; Yaghoubi, M.; Najjaran, H. Intelligent manufacturing execution systems: A systematic review. *J. Manuf. Syst.* **2022**, *62*, 503–522. [CrossRef]
2. Villani, V.; Pini, F.; Leali, F.; Secchi, C. Survey on humanrobot collaboration in industrial settings: Safety, intuitive interfaces and applications. *Mechatronics* **2018**, *55*, 248–266. [CrossRef]
3. Liu, Q.; Liu, M.; Zhou, H.L.; Yan, F.; Ma, Y.Y.; Shen, W.M. Intelligent manufacturing system with human-cyber-physical fusion and collaboration for process fine control. *J. Manuf. Syst.* **2022**, *64*, 149–169. [CrossRef]
4. Ding, H.; Kain, S.; Schiller, F.; Stursberg, O. Increasing Reliability of Intelligent Manufacturing Systems by Adaptive Optimization and Safety Supervision. In Proceedings of the 7th IFAC Symposium on Fault Detection, Supervision and Safety of Technical Processes, Barcelona, Spain, 30 June–3 July 2009.
5. Fana, C.F.; Chana, C.C.; Yua, H.Y.; Yih, S. A simulation platform for human-machine interaction safety analysis of cyber-physical systems. *Int. J. Ind. Ergon.* **2018**, *68*, 89–100. [CrossRef]
6. Hanna, A.; Larsson, S.; Götvall, P.; Bengtsson, K. Deliberative safety for industrial intelligent human–robot collaboration: Regulatory challenges and solutions for taking the next step towards industry 4.0. *Robot. Comput. Integr. Manuf.* **2022**, *78*, 102386. [CrossRef]
7. Gerakios, P.; Papaspyrou, N.; Sagonas, K. Static safety guarantees for a low-level multithreaded language with regions. *Sci. Comput. Program.* **2014**, *80*, 223–263. [CrossRef]
8. Xia, C.Y.; Xia, H.; Roeck, G.D. Dynamic response of a train–bridge system under collision loads and running safety evaluation of high-speed trains. *Comput. Struct.* **2014**, *140*, 23–38. [CrossRef]
9. Fan, Z.; Jiang, S.; Zhang, M. Dynamic probability evaluation of safety levels of earth-rockfill dams using Bayesian approach. *Water Sci. Eng.* **2009**, *2*, 61–70.
10. Samosir, A.S.; Yatim, A.H.M. Dynamic evolution control for synchronous buck DC-DC converter: Theory, model and simulation. *Simul. Model. Pract. Theory* **2010**, *18*, 663–676. [CrossRef]
11. Han, D.; Shi, P.; Zhou, G.; Li, Z.; Li, X.; Wang, L. Safety Evaluation of Marine Derrick Steel Structures Based on Dynamic Measurement and Updated Finite Element Model. *Procedia Eng.* **2011**, *26*, 1891–1900.
12. Oyewole, S.A.; Farde, A.M.; Haight, J.M.; Okareh, O.T. Evaluation of complex and dynamic safety tasks in human learning using the ACT-R and SOAR skill acquisition theories. *Comput. Hum. Behav.* **2011**, *27*, 1984–1995. [CrossRef]
13. Guastello, S.J. Nonlinear dynamics, complex systems and occupational accidents. *Hum. Factors Ergon. Manuf.* **2003**, *13*, 293–304. [CrossRef]
14. Orfila, O.; Coiret, A.; Do, M.T.; Mammar, S. Modeling of dynamic vehicle–road interactions for safety-related road evaluation. *Accid. Anal. Prev.* **2010**, *42*, 1736–1743. [CrossRef] [PubMed]
15. Scheuerer, M.; Heitsch, M.; Menter, F.; Egorov, Y.; Toth, I.; Bestion, D.; Pigny, S.; Paillere, H.; Martin, A.; Boucker, M.; et al. Evaluation of computational fluid dynamic methods for reactor safety analysis (ECORA). *Nucl. Eng. Des.* **2005**, *235*, 359–368. [CrossRef]
16. Zhou, M.Z.; Hu, L.L.; Chen, S.R.; Zhao, X. Different mechanical-electrochemical coupled failure mechanism and safety evaluation of lithium-ion pouch cells under dynamic and quasi-static mechanical abuse. *J. Power Sources* **2021**, *497*, 229897. [CrossRef]
17. Li, J.J.; Yu, A.Q.; Xu, B.W. Risk propagation and evolution analysis of multi-level handlings at automated terminals based on double-layer dynamic network model. *Phys. A Stat. Mech. Its Appl.* **2022**, *605*, 127963. [CrossRef]
18. Findler, N.V. A predictive man-machine environment for training and evaluating control operators. *Eng. Appl. Artif. Intell.* **2002**, *5*, 441–450. [CrossRef]
19. Proctor, C.L.; Khalid, T.M. A quantitative approach to performance evaluation of man-machine systems having a stochastic environment. *Int. J. Man Mach. Stud.* **2000**, *3*, 127–140. [CrossRef]
20. Haimson, B. Micromechanisms of borehole instability leading to breakouts in rocks. *Int. J. Rock Mech. Min. Sci.* **2007**, *44*, 157–173. [CrossRef]

21. Hu, Y.X.; Li, X.B. Bayes discriminant analysis method to identify risky of complicated goaf in mines and its application. *Trans. Nonferrous Met. Soc. China* **2012**, *22*, 425–431. [CrossRef]
22. Han, M. Bifurcations of periodic solutions of delay differential formulas. *J. Differ. Formulas* **2003**, *189*, 396–411.
23. Walther, H.O. A periodic solution of a differential formula with state-dependent delay. *J. Differ. Formulas* **2008**, *244*, 1910–1945.
24. Walther, H.O. The solution manifold and C1-smoothness for differential formulas with state-dependent delay. *J. Differ. Formulas* **2003**, *195*, 46–65.
25. Mallet-Paret, J.; Nussbaum, R.D. Superstability and rigorous asymptotics in singularly perturbed state-dependent delay-differential formulas. *J. Differ. Formulas* **2011**, *250*, 4037–4084.
26. Bentley, T.A.; Parker, R.J.; Ashby, L.; Moore, D.J.; Tappin, D.C. The role of the New Zealand forest industry injury surveillance system in a strategic Ergonomics, Safety and Health Research Programme. *Appl. Ergon.* **2002**, *33*, 395–403. [CrossRef]
27. Guadix, J.; Carrillo-Castrillo, J.; Onieva, L.; Lucena, D. Strategies for psychosocial risk management in manufacturing. *J. Bus. Res.* **2015**, *68*, 1475–1480. [CrossRef]
28. Babloyantz, A.; Lourenço, C.; Sepulchre, J.A. Control of chaos in delay differential formulas, in a network of oscillators and in model cortex. *Phys. D Nonlinear Phenom.* **1995**, *86*, 274–283. [CrossRef]
29. Zuo, H.; Luo, Z.; Wu, C. Classification identification on acoustic emission signals from underground metal mine rock by ICIMF classifier. *Math. Probl. Eng.* **2014**, *2014*, 524304. [CrossRef]
30. Wang, S.; Zuo, H. Safety diagnosis on coal mine production system based on fuzzy logic inference. *J. Cent. South Univ.* **2012**, *19*, 477–481. [CrossRef]
31. Hota, H.S.; Sanjay, K.S.; Ragini, S. Application of Fuzzy Analytic Hierarchy Method in Software Engineering Scenario. *Int. J. Comput. Appl.* **2012**, *57*, 45–50.